References

BENDERSKY, L. (1985). *Phys. Rev. Lett.* **55**, 1461–1463.
HIRABAYASHI, M. & HIRAGA, K. (1987). *Mater. Sci. Forum*, **22/24**, 45–54.
JANSSEN, T. (1986). *Acta Cryst.* A**42**, 261–271.
JARIC, M. V. (1986). *Phys. Rev. B*, **34**, 4685–4698.
KONTIO, A., STEVENS, E. D., COPPENS, P., BROWN, R. D., DWIGHT, A. E. & WILLIAMS, J. M. (1978). *Acta Cryst.* B**36**, 435–436.
LI, X. Z. (1995). *Acta Cryst.* B**51**, 265–270.
LI, X. Z., DUBOIS, J. M. & KUO, K. H. (1994). *Philos. Mag. Lett.* **69**, 93–98.
LI, X. Z., DUNEAU, M. & KUO, K. H. (1994). *Europhys. Lett.* **26**, 589–594.
NIIZEKI, K. (1993). *Mater. Trans. JIM*, **34**, 109–115.
SHOEMAKER, C. B., KESZLER, D. A. & SHOEMAKER, D. P. (1989). *Acta Cryst.* B**45**, 13–20.
SHI, N. C., LI, X. Z., MA, Z. S. & KUO, K. H. (1994). *Acta Cryst.* B**50**, 22–30.
STEINHARDT, P. J. (1987). *Mater Sci. Forum*, **22/24**, 397–408.
STEURER, W. (1991). *J. Phys. Condens. Matter*, **3**, 3397–3410.
STEURER, W. & KUO, K. H. (1990). *Acta Cryst.* B**46**, 703–712.
TAYLOR, M. A. (1959). *Acta Cryst.* **12**, 393–396.
YAMAMOTO, A. & ISHIHARA, K. N. (1988). *Acta Cryst.* A**44**, 707–714.

Acta Cryst. (1995). B**51**, 275–287

(3 + 2)-Dimensional Superspace Approach to the Structure of the Incommensurate Intergrowth Compound: $(SbS)_{1.15}TiS_2$

BY Y. REN, A. MEETSMA, V. PETRICEK,* S. VAN SMAALEN AND G. A. WIEGERS

Chemical Physics, Materials Science Center, University of Groningen, Nijenborgh 4, 9747 AG Groningen, The Netherlands

(*Received* 8 *August* 1994; *accepted* 1 *December* 1994)

Abstract

The inorganic misfit-layer compound $(SbS)_{1.15}TiS_2$ was prepared by high-temperature reaction of the elements. The structure, determined by single-crystal X-ray diffraction, is described by two interpenetrating incommensurately modulated subsystems. The first subsystem comprises TiS_2 sandwiches, with Ti atoms in trigonal-antiprisms of S atoms. The lattice parameters are $a'_{11} = 3.403\,(1)$, $a'_{12} = 3.410\,(1)$, $a_{13}' = 11.385\,(1)$ Å, $\alpha'_1 = 81.544\,(7)$, $\beta'_1 = 82.817\,(8)$ and $\gamma'_1 = 60.08\,(1)°$. The second subsystem is built of intrinsically interface-modulated double layers of SbS. The basic structure unit-cell dimensions are given by $a'_{21} = 2.954\,(1)$, $a'_{22} = 2.968\,(1)$, $a'_{23} = 11.311\,(1)$ Å, $\alpha_2 = 83.973\,(8)$, $\beta_2 = 85.87\,(1)$, $\gamma_2 = 84.06\,(1)°$. The interface modulation wavevector of SbS is given by $\mathbf{q} = 0.409(\mathbf{a}^{*\prime}_{21} + \mathbf{a}^{*\prime}_{22})$. The two subsystems have the common $(\mathbf{a}^{*\prime}_{\nu 2}, \mathbf{a}^{*\prime}_{\nu 3})$ plane. The whole X-ray diffraction pattern is indexed with five integer indices, thus a (3 + 2)-dimensional superspace group is used to analyse the complete structure. Both the superspace-group symmetry and the subsystem symmetries are centrosymmetric triclinic, belonging to the superspace group $P\bar{1}$. Refinement on 2483 reflections with $I > 2.5\sigma(I)$ converged to $wR = 0.069$ ($R = 0.062$). The final structure model consists of both occupational and displacive modulations for the atoms in the SbS subsystem, which results in zigzag clusters of –Sb–Sb– and –S–S– parallel to the $[1\bar{1}0]$ direction of SbS. The shortest Sb—Sb and S—S distances are 2.84 and 3.43 Å, respectively. The average valence of Sb was calculated as 3.13. The distinguishing feature is the incommensurate ordering of Sb/S atoms on the rock-salt structure, with a modulation wavevector apparently unrelated to the periodicities of the TiS_2 subsystem.

1. Introduction

Recently, misfit-layer compounds $(\mathcal{MX})_{1+\delta}(\mathcal{TX}_2)_n$, ($\mathcal{M}$ = Sn, Pb, Bi, Sb, and rare earth elements; $\mathcal{T}$ = Ti, V, Cr, Nb, Ta; $\mathcal{X}$ = S, Se; $0.09 < \delta < 0.23$; $n = 1$ or 2) have attracted much attention, because of their special crystallographical features as well as many interesting physical properties (Wiegers *et al.*, 1989; Wiegers & Meerschaut, 1992; van Smaalen, 1992*a*). These compounds are built of two different types of layers: two-atom-thick ($\mathcal{MX}$) layers with a distorted NaCl-type structure and $(\mathcal{TX}_2)_n$ ($n = 1, 2$) sandwiches with a NbS_2- or TiS_2-type structure. Commonly, the layers $\mathcal{MX}$ and $\mathcal{TX}_2$ are stacked alternately, but also compounds have been found with paired sandwiches of $\mathcal{TX}_2$ (Meerschaut, Auriel & Rouxel, 1992). Structures of misfit compounds can be described by assigning different unit cells to the $\mathcal{MX}$ and $\mathcal{TX}_2$ layer types. Both unit cells have $\mathbf{c}^*$ axes in common, perpendicular to the layers, and one common $\mathbf{b}^*$ axis. The two unit cells are mutually incommensurate, as expressed by the collinear $\mathbf{a}$ axes with incommensurate length ratio. The interaction of the subsystems induces a mutual modulation, where $\mathbf{a}^*_{11}$ is the modulation wavevector of the second subsystem, and $\mathbf{a}^*_{21}$ the modulation

*Permanent address: Institute of Physics, Czech Academy of Sciences, Cukrovarnicka 10, 162 00 Praha 6, Czech Republic.

wavevector of the first. A complete description of all the structural features is only possible within the superspace approach (van Smaalen, 1992*a*; Janner & Janssen, 1980; van Smaalen, 1989; Kato, 1990; van Smaalen, 1991). With only one incommensurate direction, a (3 + 1)-dimensional superspace description has always been applied. The SbS subsystem has a structure with an interface-modulated ordering of Sb and S, replacing the usual rock-salt-type order. The modulation wavevector for this ordering is independent from the periodicities of the TiS_2 subsystem, and the structure of $(SbS)_{1.15}TiS_2$ is analysed in (3 + 2)-dimensional superspace.

For T = Ti, V or Cr, trigonal-antiprismatic coordination by S or Se results, and monoclinic or triclinic lattices are found for the two subsystems. Four possibilities for the combinations of the intralayer axes for the two subsystems were predicted [Fig. 1 (Wiegers, Meetsma, van Smaalen, Haange & de Boer, 1990)]. However, so far, only case (*d*) is reported in real structures, and the γ angles were always found to be equal to 90°. In this paper, the first example $(SbS)_{1.15}TiS_2$ is presented for case (*c*) (Fig. 1), with $\gamma(TiS_2) = 90°$ and $\gamma(SbS) = 84.06°$, being different from 90°, and being different from each other. $(SbS)_{1+\delta}TiS_2$, prepared by Gotoh, Onoda, Akimoto & Oosawa (1991), was characterized by these authors presumably as a misfit compound using [001]-zone electron diffraction; $d_{001} = 11.24$ Å from X-ray powder diffraction ($00l$ reflections only).

2. Experimental

The compound $(SbS)_{1+\delta}TiS_2$ was synthesized from the elements by high-temperature reaction. A mixture of the elements Sb, Ti and S, in the ratio expected for a misfit-layer compound with $\delta = 0.12$, was sealed in an evacuated quartz ampoule and heated in a single-zone furnace at 573 K for 2 d and at 723 K for 1 d. The ampoule was then kept at 893 K for 1 month, during which single crystals were formed. The crystals of dimensions up to $2 \times 2 \times 0.02$ mm^3 are thin platelets with a metallic lustre.

A single crystal of a parallelepiped shape of *ca* $0.2 \times 0.2 \times 0.02$ mm^3 was selected for X-ray diffraction experiments. Weissenberg photographs of the crystal clearly show diffraction due to two subsystems with common $\mathbf{b}^*, \mathbf{c}^*$ vectors. Fig. 2 shows the Weissenberg photograph and the undistorted reciprocal lattice for the

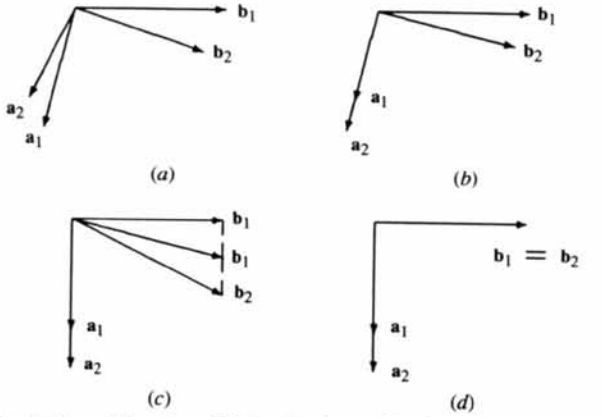

Fig. 1. Four different possibilities for the combination of the intralayer axes for the two subsystems; the axes have been given a common origin for clarity.

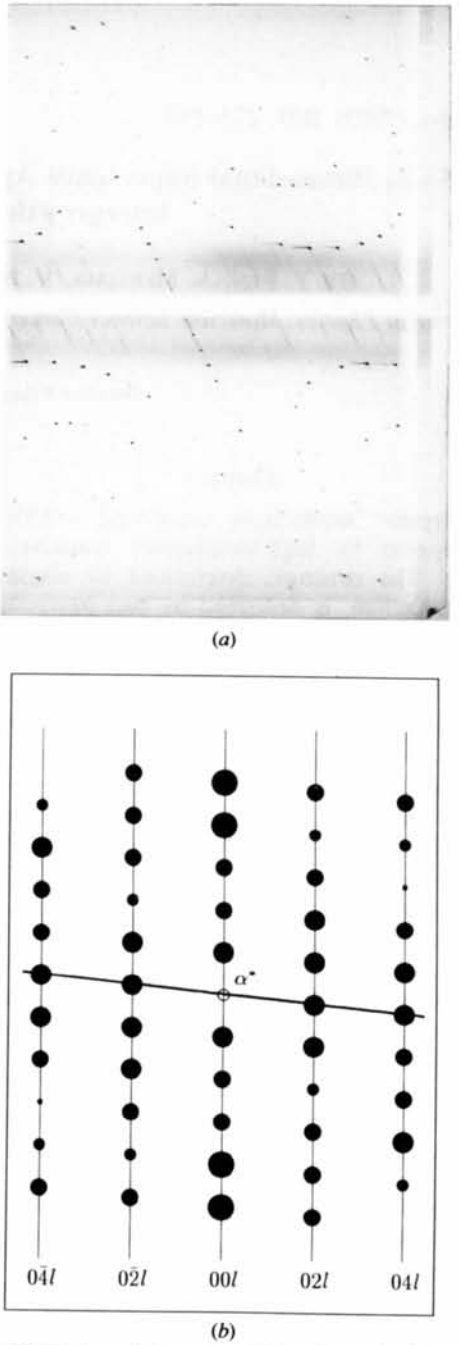

Fig. 2. (*a*) Weissenberg photograph and (*b*) undistorted reciprocal lattice of the common reflections $0kl$.

common reflections $0kl$. The TiS_2 region has a triclinic lattice similar to that found in $(SnS)_{1.20}TiS_2$ (Wiegers & Meerschaut, 1992). However, for the expected unit cell of SbS with $a_{SbS} \approx b_{SbS} \approx 5.9$ Å, only main reflections with h and k even are present. Rather than hkl reflections with h and k odd, satellites are observed along the $[110]^*$ direction. Fig. 3 shows the Weissenberg photograph and the undistorted reciprocal lattice of the main reflections hhl, together with the satellites of the SbS subsystem. The satellite reflections are as sharp as the main reflections and no diffuse intensity is found. These observations resemble those found for the Bi-containing compounds $(BiS)_{1.08}TaS_2$ (Gotoh, Onoda, Akimoto, Goto & Oosawa, 1992), $(BiSe)_{1.09}NbSe_2$ (Zhou, Meetsma, de Boer & Wiegers, 1992) and $(BiSe)_{1.10}TaSe_2$ (Petricek *et al.*, 1993). Fig. 4 illustrates the arrangement of the satellites in the $(\mathbf{a}^*, \mathbf{b}^*)$ plane of SbS. A new feature different from other misfit-layer compounds is that the γ angle between $\mathbf{a}$ and $\mathbf{b}$ of the SbS subsystem is no longer 90°.

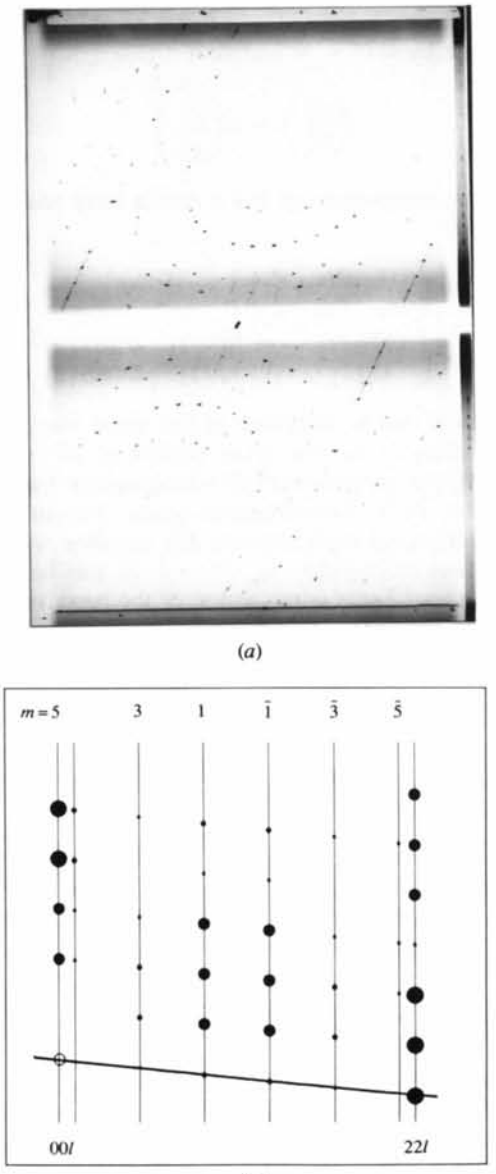

(*a*)

(*b*)

Fig. 3. (*a*) Zero-layer Weissenberg photograph and (*b*) undistorted reciprocal lattice of the crystal aligned along the $[1\bar{1}0]$ direction of SbS.

Table 1. *Unit-cell dimensions of the* TiS_2 *and* SbS *subsystems*

Subcell	ν	$a_{\nu 1}$ (Å)	$a_{\nu 2}$ (Å)	$a_{\nu 3}$ (Å)	α_ν (°)	β_ν (°)	γ_ν (°)
TiS_2	1	3.403 (1)	5.911 (1)	11.385 (1)	84.39 (1)	82.817 (8)	90.01 (1)
SbS	2	5.908 (2)	5.936 (2)	11.311 (1)	83.973 (8)	85.87 (1)	84.06 (1)

Single-crystal X-ray diffraction measurement was performed on an Enraf–Nonius CAD-4*F* diffractometer with monochromatized Mo $K\bar{\alpha}$ radiation ($\lambda = 0.71073$ Å). 25 reflections were used to determine the lattice parameters of the two subsystems. Using the program *DIRAX* (Duisenberg, 1992), most reflections could be indexed on either one of two triclinic unit cells. The remaining reflections were found to be satellites, with modulation wavevector $\mathbf{q} = 0.409(\mathbf{a}^{*\prime}_{SbS} + \mathbf{b}^{*\prime}_{SbS})$, based on the primitive SbS reciprocal lattice of main reflections.

In order to obtain more accurate values, unit-cell dimensions and their standard deviations were re-determined independently for each subsystem from the setting angles in four alternate settings of 15 reflections in the range $24.59 < \theta < 34.66°$ for TiS_2, and 21 reflections in the range $7.26 < \theta < 19.39°$ for SbS. For comparison with other misfit-layer compounds and facilitating the analysis, the fourfold unit cell ($2\mathbf{a} \times 2\mathbf{b}$ of the primitive unit cell) of the SbS subsystem is used and the TiS_2 subsystem is described in a C-centred unit cell (Table 1). The modulation wavevector $\mathbf{q}$, with respect to the basic lattice of SbS, was determined as $\mathbf{q} = 0.818(\mathbf{a}^*_{21} + \mathbf{a}^*_{22})$. From the volume ratio $2V_1/V_2$, equal to the ratio $2\mathbf{a}_{11}/\mathbf{a}_{21}$, of the subsystem unit cells, one finds that the composition of this compound is $(SbS)_{1.15}TiS_2$.

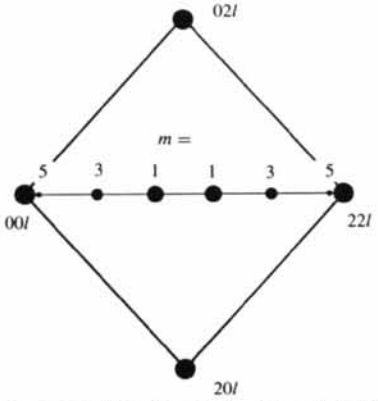

Fig. 4. Arrangement of satellites in the $(\mathbf{a}^*_{21}, \mathbf{a}^*_{22})$ plane of SbS.

Data collection was performed separately for the two subsystems using the θ–2θ scan technique. Intensities were measured at the nodes of the reciprocal lattices based on the two sets of the primitive cell dimensions. All main reflections were measured in one hemisphere up to $\theta = 35°$. The first- and third-order satellites of the interface modulation of the SbS region were measured together with its main reflections. The experimental stability was checked by the standard reflections $(\bar{1}19)$ and (013) for TiS_2 and $(01\bar{3})$ and (013) for SbS, measured every 2 h of X-ray exposure time, showing a long-term variation of less than 2%. The intensities were corrected for scale variation, Lorentz and polarization effects, and for absorption ($\mu = 98.8$ cm^{-1}) using a Gaussian integration method (Spek, 1983).

A total of 1451 reflections were measured for the TiS_2 subsystem. For the SbS subsystem 6899 reflections were measured, including 2734 first-order and 2768 third-order satellites. The common reflections ($0kl$) were used to bring the two data sets into one data set with the same scale. 145 common reflections with $I > 2.5\sigma(I)$, present in both sets, resulted in an average scale factor of 6.23 (1), which was used to multiply to the SbS intensities. The two sets of ($0kl$) reflections were averaged; 11 reflections were omitted because of a relatively large difference between their values in both data sets. The internal consistency is $R_I = 0.037$. The result was a single data set for the complete structure with 8350 reflections which were further combined into 6769 unique reflections, using Laue symmetry $\bar{1}$. The internal consistency is $R_I = (\sum_i |I_i - I_i^{av}|)/(\sum_i I_i) = 0.034$ for the observed reflections with $I > 2.5\sigma(I)$. With this criterion for observability, the number of unique reflections finally reduced to 2483, including 134 ($0kl$) reflections for the common part, 802 for the TiS_2 subsystem, 526 main reflections for SbS and 804 and 217 for the first- and third-order satellites of the SbS subsystem. Refinements on this data set were carried out with the computer program system *JANA93* (Petricek, 1993). Plots of the interatomic distances and bond valences as functions of the internal coordinates (t_1, t_2) have been made with the program *MISTEK* (van Smaalen, 1993).

3. Superspace symmetry

Intergrowth compounds are aperiodic crystals, characterized by the presence of two or more interpenetrating periodic structures. Their interaction makes each subsystem an incommensurate modulated structure. Inorganic misfit-layer compounds are one class of composite structures, consisting of two layered structures of different chemical composition. The diffraction patterns always show two sets of strong reflections which belong to the two basic structure reciprocal lattices. Weak satellite reflections are present, due to the mutual interaction. So-called *antiphase boundaries* have been found in Bi-containing misfit-layer compounds, resulting in strong satellite reflections. Such a phenomenon occurs again in $(SbS)_{1.15}TiS_2$, but with the wavelength of the antiphase boundary structure incommensurate with the TiS_2 lattice.

The complete diffraction pattern of $(SbS)_{1.15}TiS_2$ can be indexed using five integer indices (H, K, L, M_1, M_2) with respect to a set of (3 + 2) basis vectors: $\mathbf{M}^* = (\mathbf{a}_1^*, ..., \mathbf{a}_5^*)$. The first three vectors are chosen as the three reciprocal basis vectors of the TiS_2 subsystem (which is chosen as the first subsystem, $\nu = 1$): $\mathbf{a}_i^* = \mathbf{a}_{1i}^*$ for $i = 1, 2, 3$. The fourth and fifth vectors are chosen as $\mathbf{a}_4^* = \mathbf{a}_{21}^*$ ($\mathbf{a}^*$ axis of the SbS subsystem, which is the second subsystem, $\nu = 2$), and $\mathbf{a}_5^* = \mathbf{q}$ describing the interface modulation in the SbS subsystem. The last two vectors can be expressed as a linear combination of the first three by a (2 × 3) matrix σ

$$\begin{pmatrix} \mathbf{a}_4^* \\ \mathbf{a}_5^* \end{pmatrix} = \sigma \begin{pmatrix} \mathbf{a}_1^* \\ \mathbf{a}_2^* \\ \mathbf{a}_3^* \end{pmatrix}, \tag{1}$$

where the components of the σ matrix have been determined as

$$\sigma = \begin{pmatrix} \sigma_{11} & \sigma_{12} & \sigma_{13} \\ \sigma_{21} & \sigma_{22} & \sigma_{23} \end{pmatrix} = \begin{pmatrix} 0.576\,(1) & -0.105\,(2) & 0.102\,(2) \\ 0.471\,(1) & 0.732\,(2) & 0.085\,(2) \end{pmatrix}. \tag{2}$$

Superspace can be obtained in the usual way, by the identification of the five basis vectors of $\mathbf{M}^*$ with the perpendicular projection of five independent translation vectors in (3 + 2)-dimensional space. For subsystem ν, the reciprocal basis vectors $\mathbf{\Lambda}_\nu^*$, together with their modulation wavevectors $\mathbf{q}_{\nu i}$ ($i = 1, 2$), can be written as an integral linear combination of the basis vectors in $\mathbf{M}^*$ (van Smaalen, 1992*a*)

$$\begin{pmatrix} \mathbf{a}_{\nu 1}^* \\ \mathbf{a}_{\nu 2}^* \\ \mathbf{a}_{\nu 3}^* \\ \mathbf{q}_{\nu 1}^* \\ \mathbf{q}_{\nu 2}^* \end{pmatrix} = \mathcal{W} \begin{pmatrix} \mathbf{a}_1^* \\ \mathbf{a}_2^* \\ \mathbf{a}_3^* \\ \mathbf{a}_4^* \\ \mathbf{a}_5^* \end{pmatrix}. \tag{3}$$

where the (5 × 5) matrix $\mathcal{W}^\nu$ can be written as a juxtaposition of a (3 × 5) ($\mathcal{Z}^\nu$) and a (2 × 5) matrix ($\mathcal{V}^\nu$), which extract the basis vectors of the basic structures and the modulation wavevectors, respectively

$$\mathcal{W}^\nu = \begin{pmatrix} \mathcal{Z}^\nu \\ \mathcal{V}^\nu \end{pmatrix} = \begin{pmatrix} \mathcal{Z}_3^\nu & \mathcal{Z}_d^\nu \\ \mathcal{V}_3^\nu & \mathcal{V}_d^\nu \end{pmatrix}. \tag{4}$$

For further application, the (3 × 5) matrix $\mathcal{Z}^\nu$ is expressed as a juxtaposition of a (3 × 3) ($\mathcal{Z}_3^\nu$) and a (3 × 2) matrix ($\mathcal{Z}_d^\nu$), and the (2 × 5) matrix $\mathcal{V}^\nu$ as a juxtaposition of a (2 × 3) matrix ($\mathcal{V}_3^\nu$) and a (2 × 2) matrix ($\mathcal{V}_d^\nu$). The $\mathcal{W}^\nu$ matrices define a coordinate transformation between superspace based on $\mathbf{M}^*$ and subsystem superspace based on $\mathbf{\Lambda}_\nu^*$ and $\mathbf{q}_{\nu i}$ ($i = 1, 2$) for each subsystem.

For the present study, the following matrices are used

$$\mathcal{W}^1 = \begin{pmatrix} 1 & 0 & 0 & 0 & 0 \\ 0 & 1 & 0 & 0 & 0 \\ 0 & 0 & 1 & 0 & 0 \\ 0 & 0 & 0 & 1 & 0 \\ 0 & 0 & 0 & 0 & 1 \end{pmatrix},$$

$$\mathcal{W}^2 = \begin{pmatrix} 0 & 0 & 0 & 1 & 0 \\ 0 & 1 & 0 & 0 & 0 \\ 0 & 0 & 1 & 0 & 0 \\ 1 & 0 & 0 & 0 & 0 \\ 0 & 0 & 0 & 0 & 1 \end{pmatrix}. \quad (5)$$

From the above expressions, one can see that each subsystem is modulated with the mutual modulation wavevector given by the periodicity along the $\mathbf{a}^*$ axis of the other subsystem, and with a common modulation wave vector $\mathbf{q}$ which has different expressions when based on the basis vectors, Λ^*_ν, of the two subsystems. For both subsystems, the basic structures have triclinic symmetry. Systematic extinction conditions were found for the (H, K, L, M_1, M_2) reflections as $H + K + M_1 =$ odd are absent. It implies a C-centring translation

$$(\tfrac{1}{2}, \tfrac{1}{2}, 0, \tfrac{1}{2}, 0). \quad (6)$$

For a centrosymmetric triclinic structure, there is one possible superspace group

$$G_s = C\bar{1}(\sigma_{11}, \sigma_{12}, \sigma_{13}; \sigma_{21}, \sigma_{22}, \sigma_{23}), \quad (7)$$

with a tentative symbol C representing the centring translation as given by (6). With the coordinate transformations defined by the matrices $\mathcal{W}^\nu$, the elements $(R^\nu_s|\tau^\nu_s)$ of the subsystem superspace groups can be derived as (van Smaalen, 1991)

$$\begin{aligned} R^\nu_s &= \mathcal{W}^\nu R_s (\mathcal{W}^\nu)^{\text{inv}} \\ \tau^\nu_s &= \mathcal{W}^\nu \tau_s, \end{aligned} \quad (8)$$

where R_s and τ_s represent the rotation and translation operations, respectively, of superspace group G_s. With $\mathcal{W}^1$ the identity, the subsystem superspace group of the first subsystem G^1_s is identical with the superspace group G_s. For the second subsystem, the subsystem superspace group is again the same as G_s

$$G^2_s = C\bar{1}(\sigma'_{11}, \sigma'_{12}, \sigma'_{13}; \sigma'_{21}, \sigma'_{22}, \sigma'_{23}), \quad (9)$$

with the same centring translation C as given by (6). However, a non-trivial transformation occurs of translations, and of the modulation wavevectors

$$\begin{aligned} \sigma^2 &= \begin{pmatrix} \sigma'_{11} & \sigma'_{12} & \sigma'_{13} \\ \sigma'_{21} & \sigma'_{22} & \sigma'_{23} \end{pmatrix} \\ &= (\mathcal{V}^2_3 + \mathcal{V}^2_d \sigma)(\mathcal{Z}^2_3 + \mathcal{Z}^2_d \sigma)^{\text{inv}} \\ &= (1/\sigma_{11}) \\ &\quad \begin{pmatrix} 1 & \sigma_{12} & \sigma_{13} \\ \sigma_{21} & \sigma_{11}\sigma_{12} - \sigma_{21}\sigma_{12} & \sigma_{11}\sigma_{23} - \sigma_{21}\sigma_{13} \end{pmatrix} \\ &= \begin{pmatrix} 1.737 & 0.182 & -0.180 \\ 0.818 & 0.818 & 0.000 \end{pmatrix}. \end{aligned} \quad (10)$$

The space groups describing the symmetry of the basic structure of each subsystem can be obtained as the restriction of G^ν_s to three-dimensional physical space: $G_1 = G_2 = C\bar{1}$ with C representing the normal C-centring translation $(\frac{1}{2}, \frac{1}{2}, 0)$.

4. The structure in superspace

In the composite structure of the misfit-layer compound $(SbS)_{1.15}TiS_2$, the coordinates of each atom μ can be specified with respect to the subsystem lattice basis $\mathbf{\Lambda}_\nu$, to which this atom belongs

$$x_{\nu i}(\mu) = \bar{x}_{\nu i}(\mu) + u^\mu_{\nu i}(\bar{x}_{\nu s4}, \bar{x}_{\nu s5}), \quad (11)$$

for $\nu = 1, 2$ and $i = 1, 2, 3$. $u^\mu_{\nu i}$ are the displacive modulation functions for atom μ with periodicities of 1 both in $\bar{x}_{\nu s4}$ and $\bar{x}_{\nu s5}$, the fourth and fifth subsystem-superspace coordinate. Let $\mathbf{t} = (t_1, t_2)$ be the set of two real numbers characterizing a particular section of superspace describing physical space. In the incommensurate case, each section $\mathbf{t}$ gives an equivalent description of physical space. The average structure coordinates $\bar{x}_{\nu i}$ can be written as (van Smaalen, 1992*a*)

$$\begin{aligned} &\bar{x}_{1i}(\mu) = n_{1i} + x^0_{1i}(\mu), \quad i = 1, 2, 3; \\ &\bar{x}_{21}(\mu) = n_{21} + x^0_{21}(\mu) - t_1; \\ &\bar{x}_{2i}(\mu) = n_{2i} + x^0_{2i}(\mu), \quad i = 2, 3; \end{aligned} \quad (12)$$

where $n_{\nu i}$ runs over all integers. The coordinates $x^0_{\nu i}(\mu)$ of atom μ with respect to its own subsystem unit cell are to be determined in the structure refinement. The fourth and fifth subsystem-superspace coordinates can be expressed as (van Smaalen, 1992*a*)

$$\begin{pmatrix} \bar{x}_{\nu s4}(\mu) \\ \bar{x}_{\nu s5}(\mu) \end{pmatrix} = \sigma^\nu \begin{pmatrix} \bar{x}_{\nu 1}(\mu) \\ \bar{x}_{\nu 2}(\mu) \\ \bar{x}_{\nu 3}(\mu) \end{pmatrix} + \mathcal{V}^\nu_d \begin{pmatrix} t_1 \\ t_2 \end{pmatrix}. \quad (13)$$

Phase $\mathbf{t}_\nu$ of the modulation functions of each subsystem is implicitly contained in (12) and (13), and amounts to

$$\mathbf{t}_\nu = (\mathcal{V}^\nu_d - \sigma^\nu \mathcal{Z}^\nu_d)\mathbf{t}. \quad (14)$$

Using the transformation matrices $\mathcal{W}^\nu$, one finds that $\mathbf{t}_1 = \mathbf{t}$ and

$$\begin{aligned} \mathbf{t}_2 = \begin{pmatrix} t_{21} \\ t_{22} \end{pmatrix} &= \begin{pmatrix} -\sigma'_{11} & 0 \\ -\sigma'_{21} & 1 \end{pmatrix} \begin{pmatrix} t_1 \\ t_2 \end{pmatrix} \\ &= \begin{pmatrix} -1.737 t_1 \\ -0.818 t_1 + t_2 \end{pmatrix}. \end{aligned} \quad (15)$$

The complete structure of $(SbS)_{1.15}TiS_2$ involves both displacive and occupational modulations. The coefficients of the Fourier expansions of the modulation functions are used as independent parameters in the refinements: for the displacive modulation

$$u^{\mu}_{\nu i}(\bar{x}_{\nu s4}, \bar{x}_{\nu s5}) = \sum_{n_1,n_2=0}^{\infty} [A^{\mu}_{i,n_1n_2} \sin(2\pi(n_1\bar{x}_{\nu s4} + n_2\bar{x}_{\nu s5})) + B^{\mu}_{i,n_1n_2} \cos(2\pi(n_1\bar{x}_{\nu s4} + n_2\bar{x}_{\nu s5}))], \quad (16)$$

for $i = 1, 2, 3$; and for the occupational modulation

$$P^{\mu}_{\nu} = P^{\mu}_0 + P^{\mu}_{\nu}(\bar{x}_{\nu s4}, \bar{x}_{\nu s5}) = P^{\mu}_0 + \sum_{n_1,n_2=0}^{\infty} [P^{\mu,s}_{n_1n_2} \sin(2\pi(n_1\bar{x}_{\nu s4} + n_2\bar{x}_{\nu s5})) + P^{\mu,c}_{n_1n_2} \cos(2\pi(n_1\bar{x}_{\nu s4} + n_2\bar{x}_{\nu s5}))], \quad (17)$$

excluding the term $(n_1, n_2) = (0, 0)$ in both summations.

5. Structure refinements

5.1. *The basic structure*

In the basic structure of $(SbS)_{1.15}TiS_2$, Ti is at the inversion centre at $(0, 0, 0)$, and Sb and S of SbS occupy the general position (x, y, z), with respect to its own subsystem unit cell, with an occupancy of $\frac{1}{2}$ because main reflections (hkl) of the SbS subsystem occur only for h and k even. Structure refinements were carried out step by step. First, 134 common reflections $(0KL0)$ were used to determine the common projection of the structure along the [100] direction. The basic coordinates of $(PbS)_{1.18}TiS_2$ (van Smaalen, Meetsma, Wiegers & de Boer, 1991) were chosen as starting values for the atomic positions in this refinement. A good fit resulted in $R = 0.044$ $\{wR = 0.060$ with $w = 1/[\sigma^2(|F_{obs}|) + (0.03|F_{obs}|)^2]\}$. The orthogonal projection of the average structure along the **a** axes is depicted in Fig. 5. Along the misfit **a** axes, one can recognize rows of S atoms in the TiS_2 subsystem and find that rows of Sb atoms are located in between the S rows, which leads each Sb atom to fulfil the maximum possible coordination by sulfur, between (5 + 2) and (5 + 3), depending upon its position along the **a** axes.

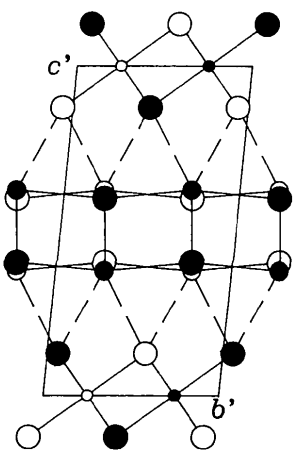

Fig. 5. Orthogonal projection of the structure of $(SbS)_{1.15}TiS_2$ along the common [100] direction; $b' = a_{\nu 2}\sin\gamma_{\nu}$ and $c' = a_{\nu 3}\sin\gamma_{\nu}$ for $\nu = 1, 2$. Large open and filled circles denote S atoms, small open and filled circles denote Ti atoms and middle ones denote Sb atoms.

After the determination of the common part, the basic structures of both subsystems SbS and TiS_2 were independently refined using 802 main reflections for TiS_2 and 526 main reflections for SbS, where the common reflections were discarded. In order to obtain the complete basic structure, refinements on 1642 reflections $(HKLM_10)$ were performed which converged smoothly to $R = 0.057$ $(wR = 0.70)$.*

5.2. *The modulated structure*

5.2.1. *The (3 + 2)-dimensional superspace approach.* The complete structure of $(SbS)_{1.15}TiS_2$ involves both displacive and occupational modulations, with the latter restricted to the SbS subsystem. As with the Bi-containing misfit-layer compounds, the specific pattern of satellites surrounding the extinct main reflections of the SbS part could be ascribed to an *antiphase boundary* structure in SbS. Alternatively, this can be described by an occupational modulation function. In $(BiSe)_{1.09}TaSe_2$ this was found to be a block wave, in good approximation (Petricek *et al.*, 1993). Here a significant deviation from a block wave is found, and the Fourier coefficients in (17) are retained as structural parameters.

Since only first- and third-order satellites were measured, initial refinement parameters included only Fourier amplitudes of the first- and third-order of the occupational modulation function for Sb and S(2) of SbS. The ordering of Sb and S(2) at the positions (x, y, z) with slightly different coordinates for each is restricted in such a way that the average occupancy of each site is $\frac{1}{2}$ for both Sb and S(2), and the total occupancy is 1. These conditions were firstly approximated using (17), with restrictions given by

$$P^{S(2),s}_{0,n_2} = -P^{Sb,s}_{0,n_2}, \text{ and } P^{S(2),c}_{0,n_2} = -P^{Sb,c}_{0,n_2}, \quad (18)$$

for $n_2 = 1$ and 3.

As is well known, displacive and occupational modulations exert their influence on the magnitude of the structure factor in different ways. In the case of a displacive modulation, the intensities of the nth-order

*Lists of structure factors, anisotropic thermal parameters, atomic coordinates, unit-cell dimensions, amplitudes of occupational modulation functions and displacive modulation parameters have been deposited with the IUCr (Reference: SE0161). Copies may be obtained through The Managing Editor, International Union of Crystallography, 5 Abbey Square, Chester CH1 2HU, England.

Table 2. *Reliability factors for the (initial) refinement REF-i and the final refinement REF-f in (3 + 2)-dimensional superspace*

The R-factors are defined as $R = \sum ||F_{obs}| - |F_{calc}|| / \sum |F_{obs}|$ and $wR = [\sum w(|F_{obs}| - |F_{calc}|)^2 / \sum w|F_{obs}|^2]^{1/2}$, with weights $w = 1/[\sigma^2(|F_{obs}|) + (0.03|F_{obs}|)^2]$. Partial R-factors are defined with a subset of reflections. Satellites of the order M_2 are defined as $HKLM_1M_2$ reflections.

Reflection subset	Number of reflections	REF-i R/wR	REF-f R/wR
All	2483	0.063/0.070	0.062/0.069
Main	1462	0.051/0.059	0.050/0.059
TiS_2	802	0.046/0.056	0.046/0.056
SbS	526	0.059/0.063	0.057/0.062
Common	134	0.043/0.064	0.042/0.064
$M_2 = 1$	804	0.078/0.080	0.078/0.079
$M_2 = 3$	217	0.176/0.206	0.173/0.206

Table 3. *Basic atomic coordinates as obtained by the final refinement REF-f in (3 + 2)-dimensional superspace of the modulated structure*

Coordinates refer to the subsystem lattice bases.

Atom	ν	$x^0_{\nu 1}$	$x^0_{\nu 2}$	$x^0_{\nu 3}$
Ti(1)	1	0	0	0
S(1)	1	0.4463 (2)	−0.1905 (1)	0.12715 (6)
Sb(2)	2	0.2339 (4)	−0.0236 (4)	0.6223 (2)
S(2)	2	0.2612 (15)	−0.0175 (10)	0.5980 (5)

satellites are dominated by the Fourier amplitudes up to the nth-order for relatively small displacements from the average structure, and are affected by the Fourier amplitudes with order even greater than n if the deviation from linearity becomes larger (van Aalst, den Hollander, Peterse & de Wolff, 1976). During the refinements of the complete structure, the displacive modulation parameters A^{μ}_{i,n_4n_5} and B^{μ}_{i,n_4n_5} [see (16)] were subsequently added. The displacements of Ti and S(1) of TiS_2 were found to be zero within the standard deviations and did not have a significant influence on the R-factors. Thus, in further refinements the displacive modulation as well as the occupational modulation were only applied to the SbS subsystem. Displacive Fourier amplitudes up to the fourth order of the modulation wave $\mathbf{q}_{22}$ for Sb and S(2) were employed. Some **sine** parts of the Fourier amplitudes had to be discarded to make the refinements more stable due to the too high correlations between sine and cosine amplitudes, which often occurs in the refinements of modulated structures with occupational modulation waves (van der Lee *et al.*, 1993). This may be due to the fact that the functions constituting the Fourier series of the displacive modulation functions are not well defined within those intervals of the phase (t) where the occupation probability of Sb or S(2) is zero or close to zero. Further addition of Fourier amplitudes of higher order did not improve the fit.

With the basic structure and modulation parameters as described above and a single anisotropic temperature factor for each independent atom, the refinement converged smoothly to $wR = 0.070$ ($R = 0.063$). Using the basic structure coordinates and modulation parameters as obtained from the refinement, the ordering of the occupancy of Sb and S(2) of SbS at each position was calculated. It was found that some sites were occupied by either Sb or S(2) and some were occupied by both Sb and S(2), each with a partial occupancy. The total occupancy was found to be largely deviating from 1 at some sites. This is caused by the large difference between the basic structure coordinates of Sb and S(2) and the unsuitable restriction (18) for (17). This problem can be solved by taking the difference of the basic coordinates of Sb and S(2) into account on the restrictions for (17), as given by

$$P^{S(2),s}_{0,1} = -1.021P^{Sb,s}_{0,1}, P^{S(2),c}_{0,1} = -0.204P^{Sb,c}_{0,1};$$
$$P^{S(2),s}_{0,3} = -1.194P^{Sb,s}_{0,3}, P^{S(2),c}_{0,3} = -0.157P^{Sb,c}_{0,3}. \quad (19)$$

The coefficients which determine the restrictions were obtained using an iterative procedure from the basic structure positions from the refinements. During refinements it was found that the change of the occupational modulation parameters as restricted by (19) strongly affected the basic coordinates and the displacive modulation parameters of Sb and S(2), and also improved the R-factors (Table 2). Using the restrictions for the occupational modulation parameters as given by (19), one finds the sum occupancy of Sb and S2 at nearly the same position as 1.000 ± 0.007. The final R-factor was $wR = 0.069$ ($R = 0.062$). The partial R-factors are listed in Table 2, where REF-i corresponds to the refinement with the occupational restrictions given by (18) and REF-f with the restrictions given by (19). The basic coordinates, temperature parameters and modulation parameters are summarized in Tables 3–6.

5.2.2. *Commensurate versus incommensurate* Sb/S(2) *ordering*. Within standard deviations, the modulation wavevector $\mathbf{q} = \mathbf{q}_{21} = 0.818(\mathbf{a}^*_{21} + \mathbf{a}^*_{22})$ can be approximated by the commensurate value $9/11 = 0.81818....$ To test the significance of this commensurate value, refinements should be performed using the commensurate structure-factor formalism for integration over t_{22}, not the incommensurate formalism for integration over t_{21}. Unfortunately, such an approach is not possible with the presently available refinement programs. However, since the interlayer interaction is weak and the satellites of the mutual modulation have not been obtained, the structure of the SbS subsystem can be refined separately (excluding $0kl$ reflections) in a (3 + 1)-dimensional approach, using only the **q**-type modulation.

The SbS subsystem is treated as a normally modulated structure with one modulation wavevector $\mathbf{q}_{4s}$. The basic unit cell is chosen as $\mathbf{a}_{4s1} = \frac{1}{2}\mathbf{a}_{21}, \mathbf{a}_{4s2} = \frac{1}{2}(\mathbf{a}_{22} - \mathbf{a}_{21}), \mathbf{a}_{4s3} = \mathbf{a}_{23}$. The superspace embedding then follows from four reciprocal vectors, given by

Table 4. *Final values for the temperature factors* ($Å^2$), *as obtained from the final refinement REF-f in* (3 + 2)-*dimensional superspace of the modulated structure*

Atom	ν	U_{11}	U_{22}	U_{33}	U_{12}	U_{13}	U_{23}
Ti(1)	1	0.0110 (3)	0.0071 (3)	0.0183 (4)	−0.0003 (2)	−0.0020 (3)	−0.0018 (2)
S(1)	1	0.0098 (3)	0.0054 (2)	0.0148 (3)	−0.0004 (2)	−0.0018 (3)	−0.0017 (2)
Sb(2)	2	0.0341 (9)	0.0171 (7)	0.0174 (4)	0.0041 (6)	−0.0020 (5)	−0.0009 (5)
S(2)	2	0.0077 (29)	0.0141 (16)	0.0139 (12)	−0.0001 (16)	−0.0025 (16)	−0.0020 (13)

The temperature factor appearing in the expression of the structure factor is defined by $T = \exp[-(\beta_{11}h_\nu^2 + \beta_{22}k_\nu^2 + \beta_{33}l_\nu^2 + \beta_{12}h_\nu k_\nu + \beta_{13}h_\nu l_\nu + \beta_{23}k_\nu l_\nu)]$ and $\beta_{ij} = 2\pi^2 U_{ij} a_{\nu i}^* a_{\nu j}^*$.

Table 5. *Final values for the amplitudes of the occupational modulation functions for* Sb *and* S(2) *as obtained from the final refinement REF-f in* (3 + 2)-*dimensional superspace of the modulated structure* (17)

The amplitude is calculated as $[(P_{n_1n_2}^{\mu,s})^2 + (P_{n_1n_2}^{\mu,c})^2]^{1/2}$.

Atom (μ)	n_1	n_2	$P_{n_1n_2}^{\mu,s}$	$P_{n_1n_2}^{\mu,c}$	Amplitude
Sb	0	0		0.5	0.5
	0	1	0.575 (4)	0.121 (3)	0.588 (5)
	0	3	0.097 (3)	0.064 (3)	0.116 (4)
S(2)	0	0		0.5	0.5
	0	1	−0.587 (4)	−0.0247 (6)	0.588 (4)
	0	3	−0.115 (3)	−0.0101 (4)	0.115 (3)

$\mathbf{a}_{4s1}^*, \mathbf{a}_{4s2}^*, \mathbf{a}_{4s3}^*, \mathbf{a}_{4s4}^*$, where $\mathbf{a}_{4s4} = \mathbf{q}_{4s} = 0.409\mathbf{a}_{4s1}^*$. The (3 + 1)-dimensional superspace group is $G_{4s} = P\bar{1}(0.409, 0, 0)$. The data set of the SbS subsystem is obtained by discarding the main reflections of TiS_2, as well as all the common reflections from the complete data set. The indices of reflections are changed corresponding to the new basis vectors.

For direct comparison, we first treated the vector $\mathbf{q}_{4s}$ as an incommensurate modulation wavevector. The refinement was performed step-by-step as before, and the structural model was identical to the SbS subsystem in the (3 + 2)-dimensional superspace-group description. Reasonable restrictions on the occupational parameters were found as

$$P_1^{S(2),s} = -1.019P_1^{Sb,s}, P_1^{S(2),c} = -0.317P_1^{Sb,c};$$
$$P_3^{S(2),s} = -1.184P_3^{Sb,s}, P_3^{S(2),c} = -0.298P_3^{Sb,c}, \quad (20)$$

which gives a sum occupancy 1.000 ± 0.002 of Sb and S(2) at nearly the same positions. A final refinement on 1547 reflections with $I > 2.5\sigma(I)$ converged to $wR = 0.080$ ($R = 0.073$). Partial R-factors for the main reflections and the satellites are close to those for the (3 + 2)-dimensional refinement (Tables 2 and 7). A direct comparison of R-factor values is not meaningful, because of neglecting the mutual modulation and discarding the common reflections.

From Table 5 one finds that the occupational modulation wave is not a simple block function as in the Bi-containing misfit-layer compounds, because in the Fourier expansion of the simple block function the amplitude of the third-order harmonics is one third of the first-order harmonics. For comparison, a refinement using the simple block function has been carried out, the displacive modulation parameters being the same as before. The final R-factors are much higher than those of the refinements using the Fourier series. This indicates that there is mixed occupancy of both Sb and S atoms at some positions, or that there is some disorder in the width of the domains separated by the antiphase boundaries.

In the superspace group description of modulated structures, the difference between incommensurate and commensurate cases is characterized by the internal coordinates, *i.e.* the phase parameters t of the modulation wave functions (van Smaalen, 1995). For the former, t can run continuously through space and sections with different t in superspace provide equivalent descriptions of the structure in real space, whereas t is limited to some discrete points for the latter and different sections within an interval along the internal axes describe different structures, which means one has to find a suitable t-value corresponding to the real structure. In the commensurate approach of the SbS region, such a suitable t-value can be found within any interval of 1/22 along the internal axis. Ten points of t have been chosen to perform refinements. Within the printed accuracy of three digits, only R-factors for the third-order satellites exhibited a slight variation, with a minimum at $t_0 = 0.4 \times 1/22$. This optimum value is almost equal but slightly smaller than that obtained in (3 + 1)-dimensionally incommensurate refinement (Table 7). The parameters of the structure from both refinements are similar to those obtained from the (3 + 2)-dimensionally incommensurate description. Therefore, the measured intensities do not provide a clue as to whether the modulation is commensurate 9/11 or truly incommensurate. This can be understood in the following way: in the refinements of the SbS structure, the integral over the internal coordinate $\bar{x}_4$ for the structure factor in the incommensurate case is replaced by a sum over the 11 different values in the commensurate case. Since there is no or very little overlap of reflections of different diffraction orders, the expressions of the structure factor for both cases lead to nearly identical results.

For a commensurate modulated structure the description by either a superspace group and modulation functions, or a three-dimensional space group using a supercell should be equivalent. However, the superspace approach generally requires less parameters than the supercell description (van Smaalen, 1995).

Table 6. *Displacive modulation parameters,* $A^{\mu}_{i,n_1n_2}a_{vi}$ (Å) *and* $B^{\mu}_{i,n_1n_2}a_{vi}$ (Å), *as obtained from the final refinement REF-f in* (3 + 2)*-dimensional superspace of the modulated structure* (16)

Atom (μ)	n_1	n_2	$A^{\mu}_{x,n_1n_2}a_{21}$	$A^{\mu}_{y,n_1n_2}a_{22}$	$A^{\mu}_{z,n_1n_2}a_{23}$	$B^{\mu}_{x,n_1n_2}a_{21}$	$B^{\mu}_{y,n_1n_2}a_{22}$	$B^{\mu}_{z,n_1n_2}a_{23}$
Sb(2)	1	0	−0.017 (6)	0.014 (2)	−0.005 (2)	−0.024 (7)	0.012 (2)	−0.013 (2)
	0	1	—	—	—	0.018 (3)	0.042 (3)	−0.025 (2)
	0	2	—	—	—	−0.076 (9)	0.069 (9)	0.057 (8)
	0	3	0.093 (14)	−0.132 (11)	−0.001 (14)	−0.009 (3)	0.018 (2)	−0.002 (3)
	0	4	—	—	—	0.120 (18)	−0.152 (11)	−0.036 (17)
S(2)	1	0	0.043 (28)	0.061 (11)	−0.002 (11)	0.048 (29)	0.003 (11)	0.019 (11)
	0	1	—	—	—	0.312 (7)	0.295 (5)	−0.005 (6)
	0	2	—	—	—	0.438 (32)	0.006 (19)	−0.023 (20)
	0	3	0.648 (37)	0.005 (26)	0.071 (28)	−0.031 (9)	−0.021 (8)	−0.021 (10)
	0	4	—	—	—	−0.392 (24)	−0.001 (22)	−0.063 (24)

Table 7. *Reliability factors for the refinements of the* SbS *region*

The R-factors are defined as $R = \sum ||F_{obs}| - |F_{calc}|| / \sum |F_{obs}|$ and $wR = [\sum w(|F_{obs}| - |F_{calc}|)^2 / \sum w|F_{obs}|^2]^{1/2}$, with weights $w = 1/[\sigma^2(|F_{obs}|) + (0.03|F_{obs}|)^2]$. Partial R-factors are defined with a subset of reflections. Satellites of the order $m_{4s,1}$ are defined as $h_{4s}k_{4s}l_{4s}m_{4s,1}$ reflections.

		R/wR			
	Number	Incommensurate		Commensurate	
Reflection subset	of reflections	Fourier series	Block function	$t_0 = 0$	$t_0 = 0.4 \times 1/22$
All	1547	0.073/0.080	0.086/0.106	0.073/0.080	0.073/0.080
Main	526	0.055/0.059	0.062/0.066	0.055/0.059	0.055/0.059
$m_{4s,1} = 1$	804	0.078/0.079	0.086/0.087	0.078/0.079	0.078/0.079
$m_{4s,1} = 3$	217	0.169/0.199	0.259/0.375	0.170/0.201	0.168/0.198

In the structure determination of the SbS subsystem, refinements using the supercell description failed to provide a good solution. Since the basic coordinates of the Sb and S(2) atoms of the SbS subsystem are almost equal, but not the same, and the occupational modulation is not a simple block wave, thus in the supercell the two different atoms will occupy almost the same positions with partial occupancies. To refine the occupancy together with the coordinates appeared to be impossible. This illustrates the power of the superspace approach to the commensurately modulated structures compared with a supercell description.

6. Discussion

The TiS_2 subsystem is similar to that in other TiS_2-based misfit-layer compounds. Its unit cell is triclinic and the Ti atoms are located in trigonal antiprisms of S(1) atoms. No significant mutual modulation of the S-atom positions in the TiS_2 region has been found. The Ti—S(1) interatomic distances are 2 × 2.428, 2 × 2.429 and 2 × 2.432 Å, similar to those in TiS_2, which indicate that the octahedral symmetry of the Ti ions is only slightly distorted.

As was seen in the refinements, the extra modulation of the SbS region can be interpreted as an (in)commensurate ordering of the two atoms Sb and S(2). However, the order is not perfect, and the modulation functions are not simple block waves, as seen in Fig. 6. Compared with the Bi-containing misfit-layer compounds, where the antiphase boundaries are built up by simple Bi–Bi and S–S or Se–Se pairs along the a axis of the BiS or BiSe subsystems, the Sb-containing misfit-layer compound shows as a new feature that the Sb–Sb and S–S contacts form along both a and b axes of the SbS lattice since the modulation wave $\mathbf{q}$ is along the diagonal of the SbS reciprocal lattice. Fig. 7 illustrates the formation of the antiphase boundaries in the SbS

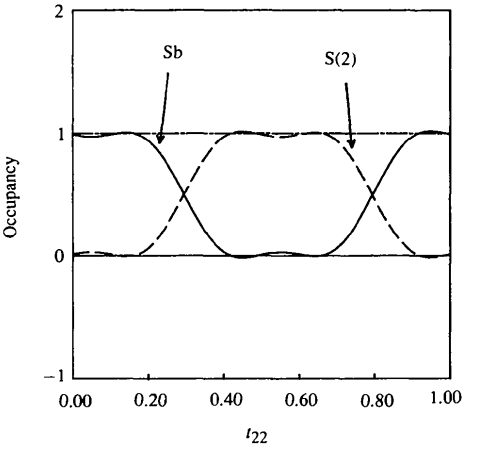

Fig. 6. Occupational modulation waves for Sb and S of SbS as a function of the phase parameter t_{22}.

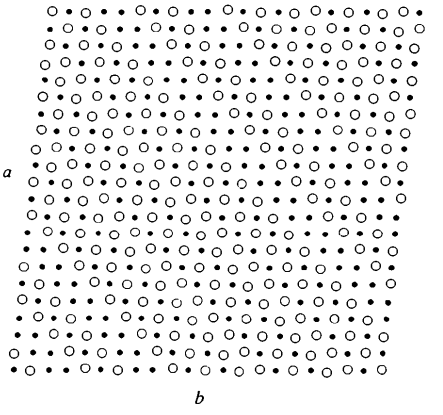

Fig. 7. One layer of the ab planes of the modulated structure of the SbS subsystem looking along the normal direction of the plane. Open circles denote S atoms and filled circles denote Sb atoms. It should be noted that in the antiphase boundaries only Sb–Sb and S–S clusters exist instead of the continuous chains, as shown here for clarity.

region on the assumption that only occupancies 1 and 0 occur for Sb and S(2) (an occupany larger than 0.6 is considered as one, otherwise as zero). In the SbS subsystem one can discern two phases which form a lamellar structure: the normal phase (denoted as the *N*-phase) has the rock-salt structure as found in other misfit-layer compounds; while the anti phase (denoted as the *A*-phase) consists of zigzag chains of Sb–Sb and S–S contacts which build up the antiphase boundaries. It is found that the partial occupation only occurs in the antiphase boundaries. The reason for the partial occupations could not be determined uniquely. Possible origins are

(i) In the *A*-phase the zigzag chains of Sb–Sb and S–S along the $[1\bar{1}0]$ diagonal of the SbS subsystem lattice are not perfect. The Sb–Sb chains are broken somewhere by S atoms, which result in Sb–Sb clusters. Considering that one Sb atom in an Sb–Sb chain is replaced by a S atom, then this S atom, together with the S atoms of the adjacent *N*-phase, will form S–S contacts as found in the S–S chains, but the nearest-neighbour Sb atoms should no longer be substituted by S atoms. The same situation occurs for the S–S chains which are broken by Sb atoms. In this case, from the structural parameters and the modulation wavefunctions (Tables 3, 5 and 6), one can establish that 22% of Sb atoms are formed in the Sb–Sb contacts.

(ii) There are perfect chains of Sb–Sb and S–S constituting two types of antiphase boundaries, but during stacking along the *c* axes each double-layered SbS shifts along the *ab* plane irregularly due to the weak interaction between two subsystems, and thus the shifts lead to the statistically partial occupation in the antiphase boundary regimes.

(iii) There are perfect chains of Sb–Sb and S–S, but the distances between adjacent antiphase boundaries are not regular. For instance, looking along the $[\bar{1}10]$ diagonal direction in Fig. 5, one row of the Sb atoms of an Sb–Sb chain may be replaced by one row of S, and this S row forms a new S–S chain with the adjacent S row of the *N*-phase. This may also occur for S–S chains where a Sb row replaced a S row to form new Sb–Sb chains.

In both cases (i) and (iii), one should expect $\approx 36\%$ of Sb atoms in the Sb—Sb bonds.

From refinements one cannot decide which one is the real case, but physical measurements may provide further information. X-ray photoemission spectroscopy (XPS) performed on a single crystal of $(SbS)_{1.15}TiS_2$ shows clearly a splitting of each peak of the Sb 3*d* core levels (Ren, Haas & Wiegers, 1995). The splitting is 1.1 eV and the Sb atoms have two different electronic states: one is trivalent and the other has metallic-like behaviour. The area ratio (3.65) of the two peaks indicates that 22% of Sb are involved in the metallic-like states. This XPS result strongly supports case (i) that the antiphase boundaries consist of clusters of Sb–Sb and S–S contacts with 22% of the Sb atoms in the Sb—Sb bonds, rather than continuous chains with $\approx 36\%$ of Sb in the Sb—Sb bonds.

Table 8. *Selected interatomic distances* (Å)

The basic structure positions of the atoms are: Sb = $(x_{21}^0, x_{22}^0, x_{23}^0)$, $Sb^{x+} = (x_{21}^0 + \frac{1}{2}, x_{22}^0, x_{23}^0)$, $Sb^{x-} = (x_{21}^0 - \frac{1}{2}, x_{22}^0, x_{23}^0)$, $Sb^{y+} = (x_{21}^0, x_{22}^0 + \frac{1}{2}, x_{23}^0)$, $Sb^{y-} = (x_{21}^0, x_{22}^0 - \frac{1}{2}, x_{23}^0)$; S(2) = $(x_{21}^0, x_{22}^0, x_{23}^0)$, $S(2)^{x+} = (x_{21}^0 + \frac{1}{2}, x_{22}^0, x_{23}^0)$, $S(2)^{x-} = (x_{21}^0 - \frac{1}{2}, x_{22}^0, x_{23}^0)$, $S(2)^{y+} = (x_{21}^0, x_{22}^0 + \frac{1}{2}, x_{23}^0)$, $S(2)^{y-} = (x_{21}^0, x_{22}^0 - \frac{1}{2}, x_{23}^0)$, $S(2)^z = (\frac{1}{2} - x_{21}^0, -x_{22}^0, 1 - x_{23}^0)$; Ti(1) = $(x_{11}^0, x_{12}^0, x_{13}^0)$; S(1) = $(x_{11}^0, x_{12}^0, x_{13}^0)$, $S(1)^1 = (1 - x_{11}^0, -x_{12}^0, 1 - x_{13}^0)$, $S(1)^2 = (\frac{1}{2} - x_{11}^0, -\frac{1}{2} - x_{12}^0, 1 - x_{13}^0)$, $S(1)^3 = (-\frac{1}{2} - x_{11}^0, -\frac{1}{2} - x_{12}^0, 1 - x_{13}^0)$, $S(1)^i = (n - x_{11}^0, -x_{12}^0, 1 - x_{13}^0)$, $S(1)^{ii} = (n + \frac{1}{2} - x_{11}^0, -\frac{1}{2} - x_{12}^0, 1 - x_{13}^0)$ and the basic coordinates x_{vi}^0, corresponding to each atom, refer to Table 3.

		Modulated structure	
Atom pair	Basic structure	Normal region	Antiphase boundaries
Sb—$Sb^{x\pm}$	2.95	—	2.84–2.92
Sb—$Sb^{y\pm}$	2.97	—	2.90–2.95
S2—$S(2)^{x\pm}$	2.95	—	3.43–3.73
S2—$S(2)^{z\pm}$	2.97	—	3.53–3.66
Sb—$S(2)^{x+}$	3.11	2.62–3.24	2.48–3.46
Sb—$S(2)^{x-}$	2.82	2.62–3.16	2.62–3.37
Sb—$S(2)^{y+}$	3.01	2.66–3.10	2.60–3.41
Sb—$S(2)^{y-}$	2.96	2.59–3.16	2.59–3.32
Sb—$S(2)^z$	2.48	2.45–2.54	2.42–2.54
Ti—$S(1)^1$	2.428	2.428	2.428
Ti—$S(1)^2$	2.432	2.432	2.432
Ti—$S(1)^3$	2.429	2.429	2.429
Sb—$S(1)^i$	3.21	3.21–	3.15–
Sb—$S(1)^{ii}$	3.15	3.14–	3.07–

For the basic structure the shortest distance from a Sb to a S(1) atom of the TiS_2 subsystem is longer than Sb to S within the SbS subsystem (Table 8), similar to that observed in the Pb-, Sn- and Bi-containing misfit compounds, but different from the rare-earth misfit-layer compounds, where the intra- and intersubsystem distances are of equal magnitude. The Sb—S distances from Sb to S(2) in the *ab* plane are several tenths of an Ångstrom longer than that from Sb to S(2) at the opposite side of the double layer, which has the shortest Sb—S distance of 2.42 Å, close to that in Sb_2S_3.

The presence of the Sb–Sb and S–S contacts in the antiphase boundaries makes a straightforward interpretation of interatomic distances and bond valences difficult. For the normal region (*N*-phase) of the SbS subsystem, the distances and angles can be calculated as usual. Selected interatomic distances are listed in Table 8. The shortest distances from Sb to S in the TiS_2 region show little change, although their distribution as a function of the phase parameters t have been strongly modified due to mutual and occupational modulation (Fig. 8). The variation, due to the modulations, of the bonding distances between an Sb atom and its four nearest S atoms in the *ab* plane is much larger than the Sb—S distance along the *c* direction (Fig. 9).

For the antiphase boundaries (*A*-phase), a distance calculation is strongly correlated with the occupational modulation, because the occupancy of Sb or S varies from 0 to 1, and thus one has to discover a suitable limit for the occupancy of Sb and S(2). As shown in Fig. 7, the zigzag chains of closed circles are, in fact, occupied

by mainly Sb (occupancy larger than 0.60); chains of open circles are mainly S atoms. In order to investigate these clusters we choose 0.60 as an occupancy limit for both Sb and S(2), as assumed for Fig. 7. The shortest bonding distance in the Sb–Sb clusters is 2.84 Å along the **a** axis of SbS, whereas the shortest S—S distance in the S–S clusters is 3.43 Å, much larger than the Sb—Sb distance. This is quite similar to the antiphase boundaries of the Bi-containing misfit-layer compounds where the S—S or Se—Se distances are much longer than Bi—Bi (Gotoh, Onoda, Akimoto, Goto & Oosawa, 1992; Petricek *et al.*, 1993) The atom pair along the c axis in the SbS subsystem has the shortest distance of 2.42 Å, equal to the shortest Sb—S distance in Fülöppite [$Pb_3Sb_8S_{15}$ (Edenharter & Nowacki, 1974)]. The variation of the bonding distances in the N-phase is greater than that in the N-phase. The shortest distance from an Sb atom in the antiphase boundaries to S atoms of the TiS_2 subsystem is reduced to 3.07 Å, tending to stabilize the metallic Sb—Sb bonds.

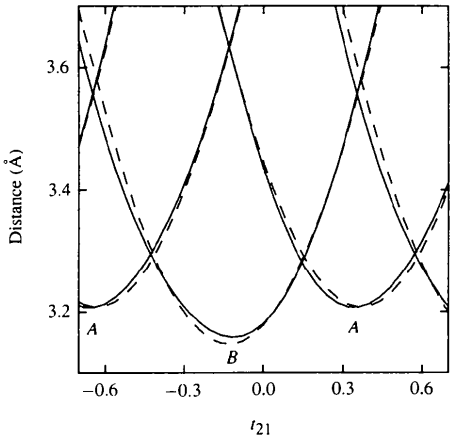

Fig. 8. Coordination of Sb ($\nu = 2$) by S(1) ($\nu = 1$) as a function of the subsystem superspace coordinate t_{21} at $t_{22} = -0.1$. Distances are given for the basic structure (broken curves) and for the modulated structure (solid lines). The curves are from Sb at $(x^0_{21}, x^0_{22}, x^0_{23})$ to S(1) at $(n_{11} - x^0_{11}, -x^0_{12}, 1 - x^0_{13})$ for the lines marked A and to S(1) at $(n_{11} + 0.5 - x^0_{11}, -0.5 - x^0_{12}, 1 - x^0_{13})$ for the curves marked B (n_{11} is an integer and $x_{\nu i}$ refers to Table 3). The curves with the same mark correspond to different values for n_{11}, but translationally equivalent S(1) atoms.

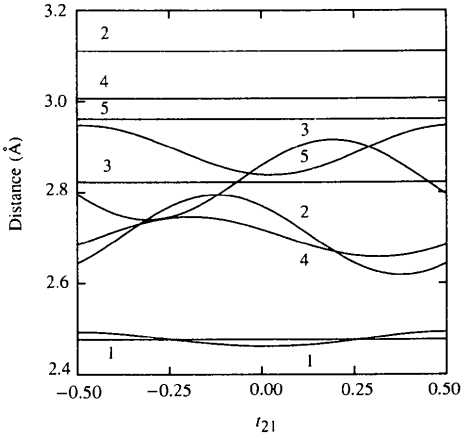

Fig. 9. Coordination of Sb ($\nu = 2$) by S(2) of the same subsystem as a function of t_{21} at $t_{22} = 0$. The distances for the basic structure are the horizontal lines and the wavy curves show the distances for the modulated structure. The curves correspond to the distance between $(E|0,0,0,0,0)$Sb and the following five symmetry equivalents of S(2): $S(2)^{x+} = (\bar{1}|0,0,1,0.5,0)S(2)$, $S(2)^{x-} = (\bar{1}|0,0,1,-0.5,0)S(2)$, $S(2)^{y+} = (\bar{1}|0,0.5,0,1,0,0)S(2)$, $S(2)^{y-} = (\bar{1}|0,-0.5,1,0,0)S(2)$, $S(2)^{z} = (\bar{1}|0,0,1,0.5,0)S(2)$. The curve and horizontal line marked 1 is the distance Sb—$S(2)^{z}$; 2 for Sb—$S(2)^{x+}$; 3 for Sb—$S(2)^{x-}$; 4 for Sb—$S(2)^{y+}$; 5 for Sb—$S(2)^{y-}$.

As is well known, the bond-valence method can quantitatively measure the bond strengths of the atoms. The valence of atom i in a structure is usually expressed as (Brown, 1981)

$$V_i = \sum_j v_{ij} = \sum_j exp[(R^0_{ij} - d_{ij})/b], \qquad (21)$$

where $b = 0.37$ Å is a constant and R^0_{ij} depends upon atoms i and j. The interatomic distance of this atom pair is d_{ij}. The summation is usually restricted to the nearest neighbours of atom i. For an incommensurately modulated structure an atom has an infinite number of bond-valence values, corresponding to an infinite number of different coordinations (van Smaalen, 1992*b*). In this new misfit-layer compound $(SbS)_{1.15}TiS_2$, due to the occupation disorder in the antiphase boundaries, it is impossible to distinguish each Sb. In order to calculate the average bond valence of Sb, the occupational modulation is introduced in (21), and the average bond valence of Sb is given by

$$\bar{V} = [\int_0^1 \int_0^1 (\sum_j v_{ij} P_i P_j) dt_{21} dt_{22}] / (\int_0^1 \int_0^1 P_i dt_{21} dt_{22}), \qquad (22)$$

where P_i and P_j are the occupancies of the Sb atom and its neighbours. Using this modified expression and parameters of $R^0_{ij} = 2.80$ Å for Sb—Sb and $R^0_{ij} =$

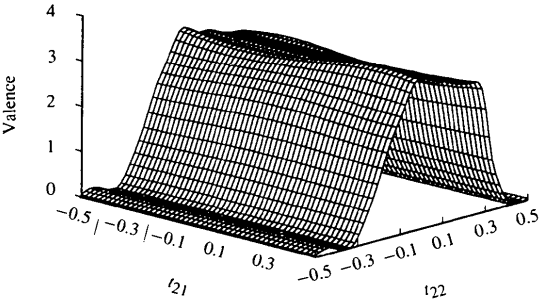

Fig. 10. Bond valence of Sb as a function of (t_{21}, t_{22}). The parameters R^0_{ij}(Sb—Sb) = 2.80, R^0_{ij}(Sb—S) = 2.45 and $b = 0.37$ Å have been used in the calculation.

2.45 Å for Sb—S (Brese & O'Keeffe, 1991), the average valence of Sb is calculated as 3.13, including 0.98 from the metallic Sb—Sb bonds, which is close to the valences of Bi and rare-earth elements in misfit-layer compounds. Fig. 10 shows the variation of the Sb bond valence as a function of the phase parameters (t_{21}, t_{22}). One can see that the bond valence of Sb *versus* t_{21} varies smoothly, and its variation as a function of t_{22} at $t_{21} = 0.0$ is illustrated in Fig. 11. The Sb—S(1) bond between the two subsystems gives a contribution of 0.21 (Fig. 12), which is close to that of the Pb atom (0.29) in O-$(PbS)_{1.18}TiS_2$ (van Smaalen, Meetsma, Wiegers & de Boer, 1991).

7. Concluding remarks

The crystal structure of the new type misfit-layer compound $(SbS)_{1.15}TiS_2$ has been studied in detail. This is the first example of a misfit-layer compound where the b axes of the two subsystems are not parallel, and with a modulation of the double-layer subsystem along its lattice diagonal. The (3 + 2)-dimensional superspace approach shows that the interface modulation of the SbS subsystem can be described by occupational modulation waves of the Sb and S atoms of SbS and the complete structure model consists of both displacive and occupational modulations. The occupational modulation wave leads to the presence of so-called *antiphase boundaries* in the SbS part, zigzagging along the $[1\bar{1}0]$ diagonal in the *ab* plane. In the antiphase boundaries, the occupational disorder results in 22% of the Sb atoms in the Sb—Sb bonds, in perfect agreement with the XPS performed on a single crystal. The distance in the Sb–Sb clusters is much smaller than the S—S distances in the S–S clusters, representing strong Sb—Sb bonds and the formation of non-bonded S–S contacts. This gives rise to a stronger displacive modulation for Sb and S(2) in the *ab* plane than along the *c* axis. The shortest Sb—S distance is 2.42 Å between an Sb atom and the S atom at opposite sides of the SbS double layers. Taking into account the occupational modulation, the average bond valence of the Sb atoms is found to be 3.13, including a contribution of 0.21 from the intersubsytem bonding between the Sb and S(1) atoms of the TiS_2 subsystem.

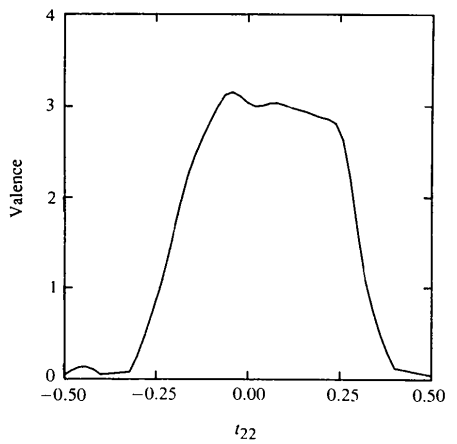

Fig. 11. Variation of the bond valence of Sb as a function of t_{22} at $t_{21} = 0$.

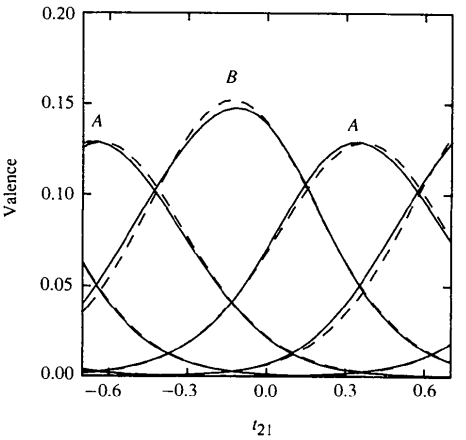

Fig. 12. Bond valences for the distances given in Fig. 8. The parameters R_{ij}^0(Sb—S) = 2.45 and b = 0.38 Å have been used in the calculation, and the occupancy of Sb is not taken into account.

The research of one of us (YR) has been made possible by financial support from the Nederlandse Organisatie voor Wetenschappelijk Onderzoek (NWO).

References

AALST, W. VAN, DEN HOLLANDER, J., PETERSE, W. J. A. M. & DE WOLFF, P. M. (1976). *Acta Cryst.* B**32**, 47–58.

BRESE, N. E. & O'KEEFFE, M. (1991). *Acta Cryst.* B**47**, 192–197.

BROWN, I. D. (1981). In *Structure and Bonding in Crystals*, Vol. 2, edited by M. O'KEEFFE & A. NAVROTSKY. New York: Academic Press.

DUISENBERG, A. J. M. (1992). *J. Appl. Cryst.* **25**, 92–96.

EDENHARTER, A. & NOWACKI, W. (1974). *Neues Jb. Miner. Mh.* 92–94.

GOTOH, Y., ONODA, M., AKIMOTO, J., GOTO, M. & OOSAWA, Y. (1992). *Jpn. J. Appl. Phys.* **31**, 3946–3950.

GOTOH, Y., ONODA, M., AKIMOTO, J. & OOSAWA, Y. (1991). *Jpn. J. Appl. Phys.* **30**, L1039–L1041.

JANNER, A. & JANSSEN, T. (1980). *Acta Cryst.* A**36**, 408–415.

KATO, K. (1990). *Acta Cryst.* B**46**, 39–44.

LEE, A. VAN DER, EVAIN, M., MONCONDUIT, L., BREC, R., ROUXEL, J. & PETRICEK, V. (1993). In the press.

MEERSCHAUT, A., AURIEL, C. & ROUXEL, J. (1992). *J. Alloys Comp.* **183**, 129–137.

PETRICEK, V. (1993). *JANA93 Programs for Modulated and Composite Crystals*. Institute of Physics, Praha, Czech Republic.

PETRICEK, V., CISAROVA, I., DE BOER, J. L., ZHOU, W. Y., MEETSMA, A., WIEGERS, G. A. & VAN SMAALEN, S. (1993). *Acta Cryst.* B**49**, 258–266.

REN, Y., HAAS, C. & WIEGERS, G. A. (1995). *J. Phys. Condens. Matter.* Submitted.

SMAALEN, S. VAN (1989). *J. Phys. Condens. Matter*, **1**, 2791–2800.

SMAALEN, S. VAN (1991). *Phys. Rev. B*, **43**, 11330–11341.

SMAALEN, S. VAN (1992*a*). In *Incommensurate Sandwiched Layered Compounds*, edited by A. MEERSCHAUT, pp. 173–222. Trans. Tech. Pub.

SMAALEN, S. VAN (1992*b*). *Acta Cryst.* A**48**, 408–410.

SMAALEN, S. VAN (1993). *MISTEK Program* (unpublished). Chemical Physics, Univ. of Groningen, The Netherlands.

SMAALEN, S. VAN (1995). *Cryst. Rev.* **4**, 79–102.

SMAALEN, S. VAN, MEETSMA, A., WIEGERS, G. A. & DE BOER, J. L. (1991). *Acta Cryst.* B**47**, 314–325.

SPEK, A. L. (1983). Proc. 8th Eur. Crystallogr. Meeting, Belgium.
WIEGERS, G. A. & MEERSCHAUT, A. (1992). In *Incommensurate Sandwiched Layered Compounds*, edited by A. MEERSCHAUT, pp. 101–172. Trans. Tech. Pub.
WIEGERS, G. A., MEETSMA, A., VAN SMAALEN, S., HAANGE, R. J. & DE BOER, J. L. (1990). *Solid State Commun.* **75**, 689–692.
WIEGERS, G. A., MEETSMA, A., VAN SMAALEN, S., HAANGE, R. J., WULFF, J., ZEINSTRA, T., DE BOER, J. L., KUYPERS, S., VAN TENDELOO, G., VAN LANDUYT, J., AMELINCKX, S., MEERSCHAUT, A., RABU, P. & ROUXEL, J. (1989). *Solid State Commun.* **70**, 409–413.
ZHOU, W. Y., MEETSMA, A., DE BOER, J. L. & WIEGERS, G. A. (1992). *Mat. Res. Bull.* **27**, 563–572.

Acta Cryst. (1995). B**51**, 287–293

Structure of Potassium Sulfate at Temperatures From 296 K Down to 15 K

BY KENJI OJIMA, YASUO NISHIHATA AND AKIKATSU SAWADA
Faculty of Science, Okayama University, Okayama 700, *Japan*

(*Received* 18 *July* 1994; *accepted* 18 *November* 1994)

Abstract

The crystal structure of potassium sulfate, K_2SO_4, was studied at five temperatures from 296 down to 15 K using an off-center four-circle diffractometer. The temperature dependence of lattice constants is well explained by the Grüneisen relation. The crystal structure is confirmed to be orthorhombic, space group *Pmcn*, down to 15 K. The S—O bond lengths in SO_4 tetrahedra with thermal motion correction are almost independent of temperature. Atomic positions of K(1), K(2) and S atoms in the β-K_2SO_4 structure are found to approach the special positions in the α-K_2SO_4 structure as temperature increases. No evidence for any phase transition has been detected below room temperature.

Introduction

Many compounds of A_2BX_4-type crystals have the β-K_2SO_4-type structure and some of these compounds have interesting features. For example, ammonium sulfate, $(NH_4)_2SO_4$, shows ferrielectric temperature dependence on spontaneous polarization (Unruh, 1970). Potassium selenate, K_2SeO_4, transforms into an incommensurately modulated phase (Iizumi, Axe & Shirane, 1977). Tetramethylammonium tetrabromocobaltate and tetramethylammonium tetrabromozincate, $[N(CH_3)_4]_2XBr_4$ (X = Zn, Co), show ferrielastic temperature dependence on monoclinic angle deviation from 90° below T_c (Hasebe, Mashiyama, Tanisaki & Gesi, 1984; Sawada, Tanaka, Matsumoto & Nishihata, 1995). Potassium sulfate, K_2SO_4, is the most fundamental crystal among the β-K_2SO_4-type crystals. Lattice constants and positional parameters at room temperature were reported by Robinson (1958) and later refined by McGinnety (1972). This crystal undergoes a first-order phase transition from the β- (orthorhombic, space group *Pmcn*) to the α-K_2SO_4 structure (hexagonal, space group $P6_3/mmc$) at high temperature. El-Kabbany (1980) reported a hysteresis with a transition temperature of 844 K on heating and 839 K on cooling. High-temperature study of the structure has been reported by van den Berg & Tuinstra (1978), Miyake, Morikawa & Iwai (1980), and Arnold, Kurtz, Richter-Zinnius, Bethke & Heger (1981). On the other hand, it was suggested from measurements of specific heat and dielectric constants that K_2SO_4 might undergo another phase transition at 56 K (Gesi, Tominaga & Urabe, 1982). The crystal structure of potassium sulfate below room temperature has not yet been reported.

The purpose of the present work is to study the crystal structure of potassium sulfate by single-crystal X-ray diffraction in the temperature range from room temperature down to 15 K. In particular, we examine whether such a phase transition really occurs.

Experiment

Single crystals of potassium sulfate were grown by slow evaporation of an aqueous solution. Integrated intensity data were measured using an off-center-type four-circle diffractometer with a χ-cradle of inner diameter 400 mm (Huber Eulerian cradle model 512), installed in the X-ray Laboratory of Okayama University. Graphite monochromatized Mo $K\alpha$ radiation was used. The shape and size of the crystal used during the experiments was spherical, diameter 0.298 (2) mm at 296, 50 and 15 K and 0.265 (2) mm at 200 and 100 K. The specimen attached to a sapphire rod was cooled by a closed-cycle helium gas refrigerator which was mounted on the φ-circle of the diffractometer. The temperature was measured by a thermocouple, Au(Fe)-chromel, attached on the supporting rod apart from the specimen by *ca* 1.5 mm. Temperature stability during the experiments was within ±0.5 at 296, 50 and 15 K, and also within ±1.0 at 200 and 100 K. Lattice parameters were refined